Instability of electromagnetic R-mode waves in a relativistic plasma

Article *in* Physics of Plasmas · July 1998

DOI: 10.1063/1.872932

3 authors, including:

Fuliang Xiao
Changsha University of Science and Technology
110 PUBLICATIONS **2,585** CITATIONS

SEE PROFILE

Instability of electromagnetic R-mode waves in a relativistic plasma

Fuliang Xiao
Department of Physics and Astronomy, University of California, Los Angeles, Los Angeles, California 90095-1547

Richard M. Thorne[a)]
Department of Atmospheric Sciences, University of California, Los Angeles, Los Angeles, California 90095-1565

Danny Summers
Department of Mathematics and Statistics, Memorial University of Newfoundland, St. John's, Newfoundland, A1C 5S7, Canada

(Received 2 February 1998; accepted 31 March 1998)

An explicit mathematical formalism is developed to evaluate the growth rate of field-aligned electromagnetic R-mode waves in a relativistic plasma. The methodology is valid for weak wave growth or damping when the resonant relativistic electrons comprise a small portion of the total plasma population. Numerical results are obtained for realistic plasma parameters using three distinct distribution functions for the relativistic electron population. Wave growth rates obtained by numerical integration along the resonant relativistic ellipse are shown to be substantially smaller than calculations performed under the nonrelativistic approximation. The relativistic corrections are primarily due to a reduction in the resonant electron anisotropy. Changes from the standard nonrelativistic treatment are noticeable at relatively small electron thermal energies (a few keV), and they become very significant for thermal energies above 100 keV, especially in low density regions where the plasma frequency is comparable to or lower than the electron gyrofrequency. The results have applications to wave instability in the outer radiation belts of the Earth, the inner Jovian magnetosphere, and other space plasmas where relativistic electrons are present. © *1998 American Institute of Physics.* [S1070-664X(98)01307-X]

I. INTRODUCTION

Electromagnetic R-mode waves with frequency below the electron gyrofrequency are an important constituent of magnetospheric plasmas. Such waves can be generated by cyclotron resonant interactions due to natural sources of free plasma energy such as those associated with a loss-cone distribution or with thermal anisotropy, which can be generated by convective injection or radial diffusion. Whistler-mode waves provide the most efficient mechanism for resonant pitch-angle scattering loss of energetic trapped electrons in the Earth's radiation belts,[1,2] and they act to limit the flux of energetic electrons in the radiation belts.[3] Natural whistler-mode emissions have been observed in the radiation belt environment of all the magnetized planets. Under certain magnetospheric conditions the cyclotron resonant energies can approach or exceed the electron rest mass energy, $m_e c^2$. An understanding of the origin of waves under such conditions requires a fully relativistic treatment.

Formal expressions from kinetic theory for the electromagnetic dielectric tensor in a relativistic plasma were given by Trubinkov[4] and Shkarofsky,[5] but the application to wave excitation was restricted to the weakly relativistic case. The weakly relativistic treatment has also been used to study the cyclotron maser instability[6–8] in the Earth's auroral zone. Sentman and Goertz[9] presented fully relativistic calculations of whistler-mode instability in the inner Jovian magnetosphere using a methodology given by Lerche.[10] Melrose[11,12] presented a general, fully relativistic growth rate formula, and also analyzed the cyclotron maser instability. A general analysis of the whistler-mode dispersion relation in a relativistic isotropic Maxwellian plasma has recently been given by Schickheiser *et al.*[13] The effects of a relativistic Maxwellian electron population on the temporal and spatial growth rates of whistler-modes has been considered by Gladd[14] and the analysis has been applied to whistler instability in laboratory plasmas. However, none of these studies has provided a detailed description of how relativistic effects modify the growth of waves in an anisotropic medium under the differing plasma conditions encountered in natural space plasmas. This is the primary goal of the present study. The general theoretical framework is described in Section II. Three distinct nonequilibrium distribution functions used to describe the source of free energy for wave growth in a relativistic plasma are presented in Section III, and numerical calculations of the wave growth rate are given in Section IV for a range of plasma parameters. Our principal conclusions are summarized in Section V.

II. GENERAL THEORY

The relativistic dispersion equation for linear, R-mode electromagnetic waves propagating parallel to a uniform magnetic field in a spatially homogeneous plasma[10,15] is

[a)]Electronic mail: rmt@atoms.ucla.edu

$$k^2=\frac{\omega^2}{c^2}+\sum_\sigma \frac{\omega_{p\sigma}^2\omega}{2c^2}\int \frac{p_\perp \hat{H} f_\sigma(p_\parallel,p_\perp)d^3p}{\gamma\omega+\Omega_\sigma-kp_\parallel}, \tag{1}$$

where $f_\sigma(p_\parallel,p_\perp)$ is the particle distribution function, $\omega_{p\sigma}=(4\pi N_\sigma q_\sigma^2/m_\sigma)^{1/2}$ is the plasma frequency, $\Omega_\sigma=q_\sigma B_o/(m_\sigma c)$ is the particle gyrofrequency, q_σ is the particle charge (sign included), N_σ is the number density, and m_σ is the rest-mass of each particle species σ, c is the speed of light, and B_0 is the magnitude of the zeroth-order magnetic field. Fourier components of the wave field ($e^{i(kx-\omega t)}$) are considered with wave number k (assumed to be real) and complex wave frequency $\omega=\omega_r+i\omega_i$; $d^3p=2\pi p_\perp dp_\parallel dp_\perp$ is the volume element in momentum space; $p=\gamma v$ is the relativistic momentum per unit mass with components $p_\parallel=\gamma v_\parallel$, $p_\perp=\gamma v_\perp$, respectively, parallel and perpendicular to the ambient magnetic field; and $\gamma=(1-v^2/c^2)^{-1/2}=(1+p^2/c^2)^{1/2}$ (with $v^2=v_\parallel^2+v_\perp^2$ and $p^2=p_\parallel^2+p_\perp^2$);

$$\hat{H}=\frac{\partial}{\partial p_\perp}+\frac{k}{\gamma\omega}\left(p_\perp\frac{\partial}{\partial p_\parallel}-p_\parallel\frac{\partial}{\partial p_\perp}\right) \tag{2}$$

is an operator in momentum space; and each particle distribution function is normalized so that

$$\int f_\sigma(p_\parallel,p_\perp)d^3p=2\pi\int_{-\infty}^{\infty}f_\sigma dp_\parallel\int_0^\infty p_\perp dp_\perp=1. \tag{3}$$

The integral in (1) is taken over all momentum space, and the poles of the integrand, given by

$$\gamma\omega+\Omega_\sigma-kp_\parallel=0, \tag{4}$$

identify the momenta of the resonant particles.

In the nonrelativistic limit ($\gamma\to1$), the operator $\hat{H}$ becomes

$$\hat{G}=\frac{\partial}{\partial v_\perp}+\frac{k}{\omega}\left(v_\perp\frac{\partial}{\partial v_\parallel}-v_\parallel\frac{\partial}{\partial v_\perp}\right), \tag{5}$$

and the dispersion equation (1) takes the form given by Kennel and Scarf;[16] see also Xue *et al.*[17] and Summers *et al.*[18]

To evaluate the growth/damping rate of R-mode waves, the standard approximation[3] is made that the plasma is comprised of a dominant cold electron population, and a small hot electron population, together with background neutralizing ions. The total electron distribution function takes the form

$$f=f_o+\nu_h f_1, \tag{6}$$

where $f_o=\delta(p_\parallel)\delta(p_\perp)/(2\pi p_\perp)$ is the cold electron distribution function, with δ the Dirac delta-function; f_1 is the hot electron distribution function to be prescribed, and $\nu_h=N_1/N_o(\ll1)$ is the density ratio between the hot and cold electron populations. When $\omega\gg\Omega_+$, the background ions make a negligible contribution to the dispersion equation (1) which can be written as

$$k^2=\frac{\omega^2}{c^2}-\frac{\omega\omega_{pe}^2}{c^2(\omega-|\Omega_e|)}+\pi\nu_h\frac{\omega_{pe}^2\omega}{c^2}\int_{-\infty}^{\infty}dp_\parallel\int_0^\infty dp_\perp\frac{p_\perp^2\hat{H}f_1}{\gamma\omega-|\Omega_e|-kp_\parallel}, \tag{7}$$

where $\omega_{pe}=(4\pi N_o e^2/m_e)^{1/2}$, and $|\Omega_e|=eB_o/(m_e c)$. In the absence of the hot electron species ($\nu_h\to0$), equation (7) reduces to the standard cold plasma dispersion equation.

By following the approach of Kennel[19] and Lerche,[10] equation (7) can be expressed in the form

$$k^2=R(\omega)+iI(\omega), \tag{8}$$

where R and I are real functions of the complex variable ω. The assumption $\nu_h\ll1$ ensures that

$$k^2\approx R(\omega_r,0)=\frac{\omega_r^2}{c^2}-\frac{\omega_r\omega_{pe}^2}{c^2(\omega_r-|\Omega_e|)}. \tag{9}$$

Furthermore, since $|\omega_i|\ll|\omega_r|$ the growth/damping rate can be obtained from

$$\omega_i\approx-I(\omega_r,0)\Big/\frac{\partial R(\omega_r,0)}{\partial\omega_r}, \tag{10}$$

where

$$I(\omega_r,0)=\pi\nu_h\frac{\omega_{pe}^2\omega_r}{c^2}\times\mathrm{Im}\left\{\int_{-\infty}^{\infty}dp_\parallel\int_0^\infty dp_\perp\frac{p_\perp^2\hat{H}f_1}{\gamma\omega_r-|\Omega_e|-kp_\parallel}\right\} \tag{11}$$

[with $\omega=\omega_r$ substituted in the expression (2) for $\hat{H}$]. It is relatively straightforward to carry out the integration with respect to $p_\parallel$ in (11), and so we omit the details of the calculation. The result is

$$\mathrm{Im}\int_{-\infty}^{\infty}dp_\parallel\frac{\hat{H}f_1}{\gamma\omega_r-|\Omega_e|-kp_\parallel}=\frac{-\pi}{k}\left[\frac{\hat{H}f_1}{\Delta_R}\right]_{p_\parallel=p_R}, \tag{12}$$

where

$$p_R=(\gamma_R\omega_r-|\Omega_e|)/k \tag{13}$$

is the resonant value of the electron parallel momentum,

$$\gamma_R=\frac{-1+(ck/\omega_r)[\{(ck/\omega_r)^2-1\}(1+p_\perp^2/c^2)(\omega_r/|\Omega_e|)^2+1]^{1/2}}{\{(ck/\omega_r)^2-1\}(\omega_r/|\Omega_e|)}, \tag{14}$$

which gives the resonant electron kinetic energy $E_k=(\gamma_R-1)m_ec^2$, and

$$\Delta_R=1-\omega_r p_R/(c^2k\gamma_R), \tag{15}$$

which can be shown to be a strictly positive quantity. The R-mode growth/damping rate can then be written as

$$\omega_i=\frac{\pi^2\nu_h\omega_{pe}^2\omega_r}{k[2\omega_r+\omega_{pe}^2|\Omega_e|/(\omega_r-|\Omega_e|)^2]} \times\int_0^\infty dp_\perp\left[\frac{p_\perp^2\hat{H}f_1}{\Delta_R}\right]_{p_\parallel=p_R}. \tag{16}$$

Before proceeding, it is useful to recover results in the nonrelativistic limit ($\gamma\to1$) where (12) takes the form

$$\mathrm{Im}\int_{-\infty}^{\infty}dv_\parallel\frac{\hat{G}f_1}{\omega_r-|\Omega_e|-kv_\parallel}=-\frac{\pi}{k}[\hat{G}f_1]_{v_\parallel=v_R}, \tag{17}$$

where

$$v_R=(\omega_r-|\Omega_e|)/k \tag{18}$$

is the resonant value of the particle velocity, and the growth/damping rate (16) can be expressed[3] in the convenient form

$$\omega_i=\frac{\pi\omega_{pe}^2\tilde{\eta}}{[2\omega_r+\omega_{pe}^2|\Omega_e|/(\omega_r-|\Omega_e|)^2]}\{\tilde{A}-A_c\}, \tag{19}$$

where

$$\tilde{A}=\left[\frac{\int_0^\infty dv_\perp v_\perp^2\left\{v_\parallel\frac{\partial f_1}{\partial v_\perp}-v_\perp\frac{\partial f_1}{\partial v_\parallel}\right\}}{2v_R\int_0^\infty dv_\perp v_\perp f_1}\right]_{v_\parallel=v_R} \tag{20}$$

is a dimensionless measure of the pitch-angle anisotropy of the resonant electrons,

$$A_c=\omega_r/(|\Omega_e|-\omega_r) \tag{21}$$

is the minimum resonant anisotropy required for instability ($\omega_i>0$), and

$$\tilde{\eta}=-2\pi\nu_h v_R\int_0^\infty dv_\perp v_\perp[f_1]_{v_\parallel=v_R} \tag{22}$$

is the fraction of the electron distribution near resonance.[3,16,17,20,21]

In the fully relativistic case, (16) can be expressed in a simple form analogous to the nonrelativistic formula (19), viz.,

$$\omega_i=\frac{\pi\omega_{pe}^2\tilde{\eta}_{rel}}{[2\omega_r+\omega_{pe}^2|\Omega_e|/(\omega_r-|\Omega_e|)^2]}\{\tilde{A}_{rel}-A_c\}, \tag{23}$$

where

$$\tilde{A}_{rel}=\frac{\frac{k}{(\omega_r-|\Omega_e|)}\int_0^\infty\frac{dp_\perp}{\Delta_R}\frac{p_\perp^2}{\gamma_R}\left[p_\perp\frac{\partial f_1}{\partial p_\parallel}-p_\parallel\frac{\partial f_1}{\partial p_\perp}\right]_{p_\parallel=p_R}}{\int_0^\infty\frac{dp_\perp}{\Delta_R}p_\perp^2\left[\frac{\partial f_1}{\partial p_\perp}\right]_{p_\parallel=p_R}} \tag{24}$$

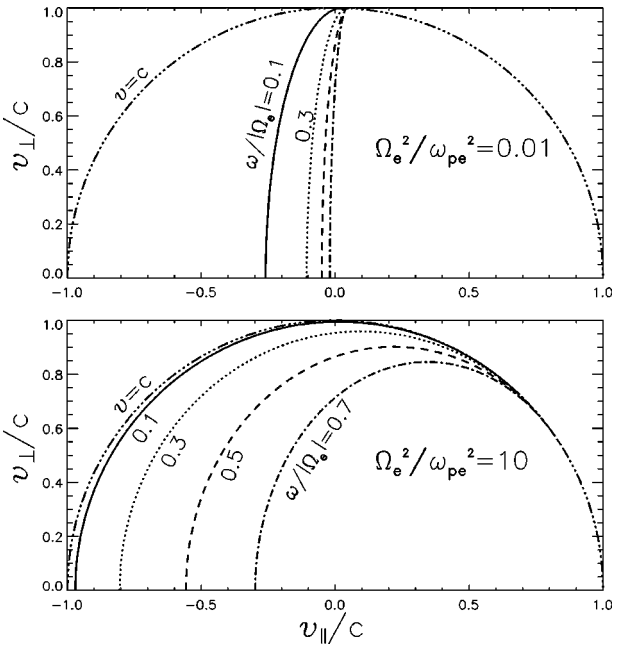

FIG. 1. Examples of the resonant ellipse in velocity space for the first-order cyclotron interaction between fully relativistic electrons and R-mode waves.

is the relativistic pitch-angle anisotropy of the resonant particles, and

$$\tilde{\eta}_{rel}=\pi\nu_h\frac{(\omega_r-|\Omega_e|)}{k}\int_0^\infty\frac{p_\perp^2dp_\perp}{\Delta_R}\left[\frac{\partial f_1}{\partial p_\perp}\right]_{p_\parallel=p_R} \tag{25}$$

is the fraction of the relativistic particle distribution near resonance. Recall that p_R, γ_R, and Δ_R are given by (13), (14), and (15), respectively. Expression (23) constitutes the principal result of this paper. The relativistic result (23) and the corresponding nonrelativistic result (19) provide expressions for the wave growth/damping rate as functions of the wave frequency ω_r, once the distribution $f_1(p_\parallel,p_\perp)$ is specified, since the wave number k can be eliminated by the use of the (real) dispersion equation (9).

Although the nonrelativistic parameters $\tilde{A}$ and $\tilde{\eta}$ [given, respectively, by (20) and (22)] can often be evaluated analytically, the relativistic parameters $\tilde{A}_{rel}$ and $\tilde{\eta}_{rel}$ must, in general, be evaluated numerically. The integrals appearing in (24) and (25) can be routinely evaluated by standard techniques of numerical quadrature, for any specified distribution function $f_1(p_\parallel,p_\perp)$.

III. DISTRIBUTION FUNCTIONS

The wave growth/damping formula (23) will be evaluated for particular relativistic distribution functions $f(p_\parallel,p_\perp)$ normalized according to (3). Standard definitions for the parallel and perpendicular mean square momenta will be adopted, namely,

$$\langle p_\parallel^2\rangle=\int p_\parallel^2 f d^3p,$$
$$\langle p_\perp^2\rangle=\int p_\perp^2 f d^3p. \tag{26}$$

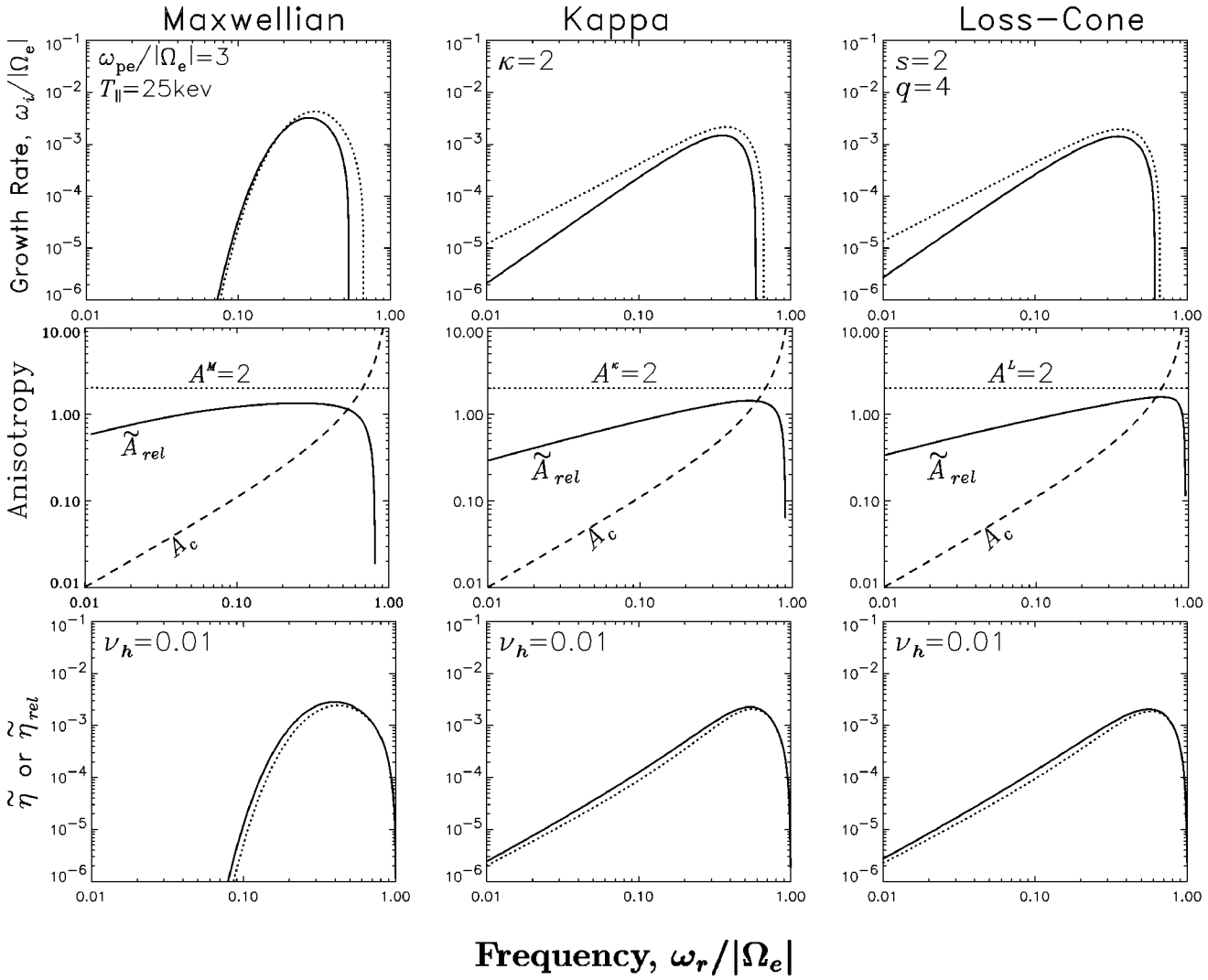

FIG. 2. The R-mode wave growth rates (top panels), relativistic electron anisotropy (middle panels), and the fractional number of resonant electrons (lower panels) for three distinct energetic electron distribution functions. Fully relativistic calculations (solid) are compared with the nonrelativistic ($\gamma\rightarrow 1$) results (dotted) for the case of a relatively high density cold population and a modest energetic electron temperature.

Relations (26) may be directly related to temperature in the nonrelativistic limit ($T_\parallel \Rightarrow m_e\langle p_\parallel^2\rangle; T_\perp \Rightarrow m_e\langle p_\perp^2\rangle/2$). Although a strict definition of temperature becomes problematic at relativistic energies, we will use (26) as a definition of ''temperature'' for a discussion of the numerical results presented in Section IV. The thermal anisotropy, which can be defined as

$$A=\frac{\langle p_\perp^2\rangle}{2\langle p_\parallel^2\rangle}-1, \tag{27}$$

provides a source of free plasma energy for wave growth. This is a natural analog to the corresponding definition ($A=T_\perp/T_\parallel-1$) in nonrelativistic theory (e.g., Summers and Thorne[22]). The relativistic distribution functions adopted in the present study are as follows.

A. Bi-Maxwellian distribution

The bi-Maxwellian distribution[23,24] is given by

$$f^M(p_\parallel,p_\perp)=\frac{1}{\pi^{3/2}a_\perp^2 a_\parallel}e^{-(p_\parallel^2/a_\parallel^2+p_\perp^2/a_\perp^2)}, \tag{28}$$

where

$$a_\parallel=(2\langle p_\parallel^2\rangle)^{1/2}, \quad a_\perp=(\langle p_\perp^2\rangle)^{1/2}, \tag{29}$$

and the thermal anisotropy is

$$A^M=\frac{a_\perp^2}{a_\parallel^2}-1. \tag{30}$$

B. Generalized Lorentzian (kappa) distribution

As a relativistic analog to the nonrelativistic generalized Lorentzian (or kappa) distribution used by various authors,[17,18,20,21,25–28] we take

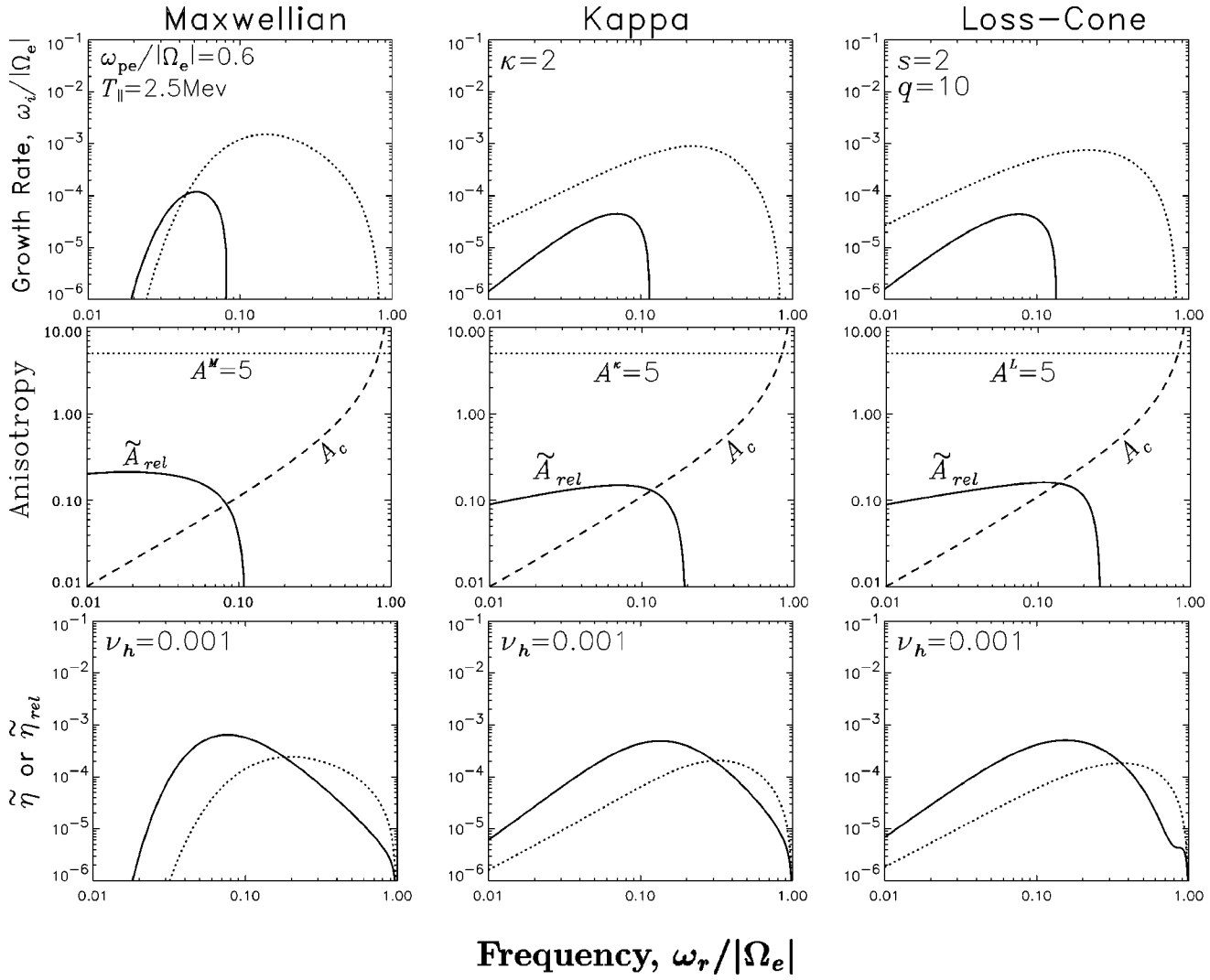

FIG. 3. Similar calculations to Figure 2, but for the case of a more tenuous cold plasma with a hot ($T_\parallel=2.5$ MeV) and highly anisotropic ($A=5$) energetic electron population.

$$f^\kappa(p_\parallel,p_\perp)=\frac{\Gamma(\kappa+1)}{\pi^{3/2}\theta_\perp^2\,\theta_\parallel\kappa^{3/2}\Gamma(\kappa-1/2)}\times\left(1+\frac{p_\parallel^2}{\kappa\theta_\parallel^2}+\frac{p_\perp^2}{\kappa\theta_\perp^2}\right)^{-(\kappa+1)} \tag{31}$$

(where Γ is the gamma function), $\kappa(>3/2)$ is the spectral index,

$$\theta_\parallel=\left(\frac{2\kappa-3}{\kappa}\right)^{1/2}(\langle p_\parallel^2\rangle)^{1/2},\theta_\perp=\left(\frac{2\kappa-3}{2\kappa}\right)^{1/2}(\langle p_\perp^2\rangle)^{1/2}, \tag{32}$$

and the thermal anisotropy is

$$A^\kappa=\frac{\theta_\perp^2}{\theta_\parallel^2}-1. \tag{33}$$

Note that if $\kappa\to\infty$, then $\theta_\parallel\to a_\parallel$, $\theta_\perp\to a_\perp$, and $f^\kappa\to f^M$, i.e., distributions (31) and (28) become identical. The kappa distribution (31) with typical values of κ in the range between 2 and 5 generally provides a better representation for the high energy tail population of natural cosmic plasmas.

C. Loss-cone distribution

Various functional forms have appeared in the literature to simulate the loss-cone particle distribution associated with a confined magnetic field geometry, e.g., see Summers and Thorne[22] and the references therein. Here, a loss-cone distribution similar to that used, for instance, by Kennel,[18] Barbosa and Coroniti,[29] Sentman and Goertz,[9] and Church and Thorne[30] is adopted, namely,

$$f^L(p_\parallel,p_\perp)=\frac{2\Gamma((q+3)/2)\Gamma(s+1)}{\pi^2p_0^3\Gamma((q+2)/2)\Gamma\left(s-\frac{1}{2}\right)}\frac{\sin^q\alpha}{(1+p^2/p_0^2)^{s+1}}, \tag{34}$$

where $\alpha=\tan^{-1}(p_\perp/p_\parallel)$ is the particle (electron) pitch-angle. Here

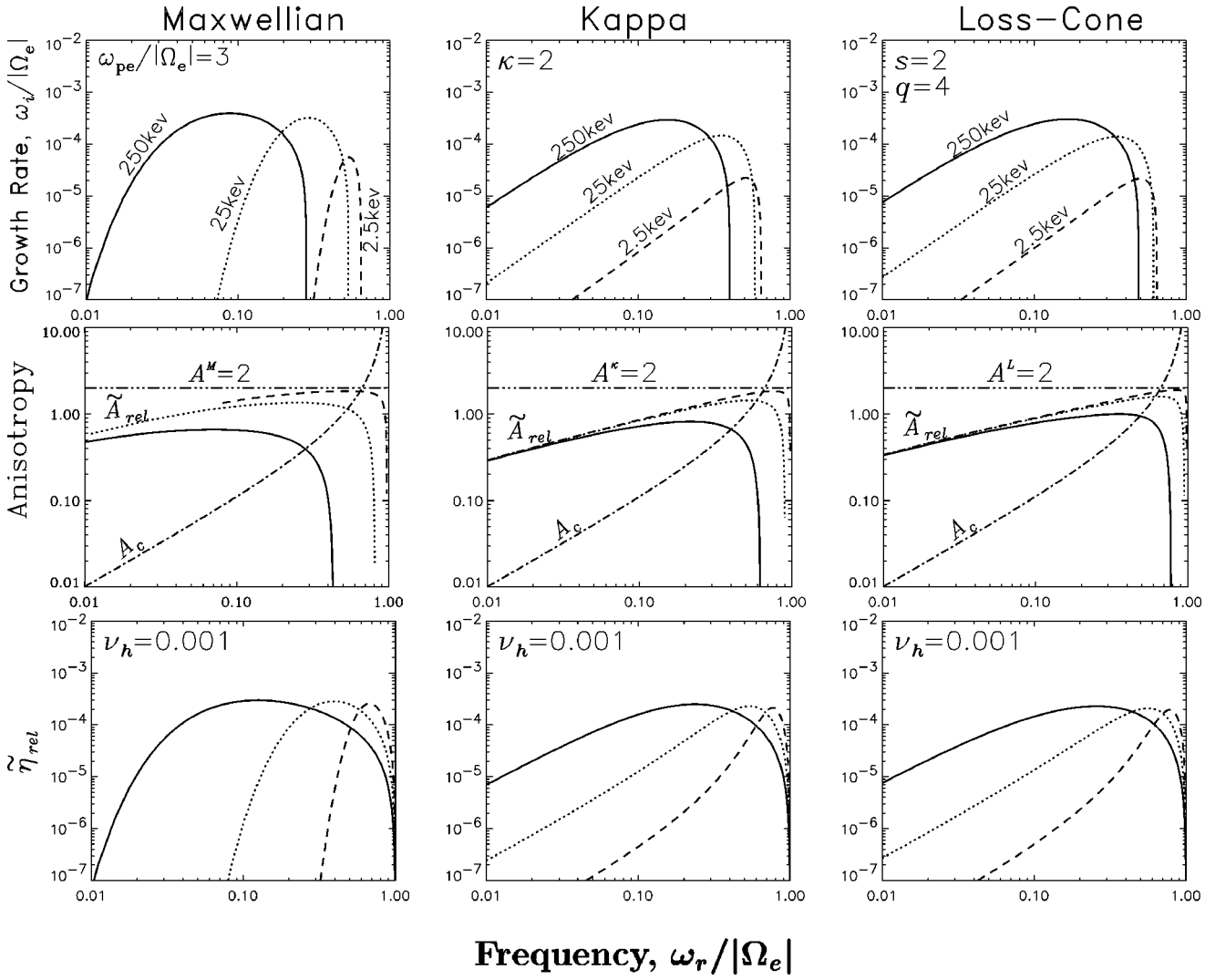

FIG. 4. Sensitivity of the fully relativistic calculations to changes in the hot electron temperature.

$$p_0=\left\{\frac{(q+3)(2s-3)}{3}\right\}^{1/2}\langle p_\parallel^2\rangle^{1/2}$$
$$=\left\{\frac{(q+3)(2s-3)}{3(q+2)}\right\}^{1/2}\langle p_\perp^2\rangle^{1/2}, \tag{35}$$

and so the temperature anisotropy is

$$A^L=\frac{q}{2}\,. \tag{36}$$

The parameter $q(>0)$, the ''loss-cone index,'' is a measure of the angular size of the loss-cone region.

IV. NUMERICAL RESULTS

The first-order cyclotron resonance between R-mode waves with frequency ω_r and fully relativistic electrons can be seen from relation (13) to be represented by an ellipse in velocity space. Figure 1 shows examples of this resonant ellipse for several specified values of $\omega_r/|\Omega_e|$, corresponding to two different magnetospheric conditions parameterized by the ratio $|\Omega_e|^2/\omega_{pe}^2$. The minimum resonant energy along each resonant curve occurs for $v_\parallel<0$, when $v_\perp=0$. There is a monotonic increase in the resonant kinetic energy (14) along each curve as $v_\perp$ increases. Resonance becomes possible with electrons moving in the same direction as the wave ($v_\parallel>0$) once the parameter γ_R exceeds the value $|\Omega_e|/\omega_r$, and the resonant ellipse touches the light curve ($\gamma_R\to\infty$) at $v_\parallel=\omega_r/k$. This behavior should be compared to the nonrelativistic case ($\gamma\to1$) in which the resonant velocity (19) is independent of $v_\perp$. Relativistic effects are particularly pronounced for low density plasmas with $|\Omega_e|>\omega_{pe}$ (lower panel).

Expression (23) for the wave growth rate can be evaluated as a function of ω_r by numerical integration of the integrals in (24) and (25) along the resonant ellipse for any specified electron distribution function. Figure 2 shows results for the case of a relatively dense plasma ($\omega_{pe}=3|\Omega_e|$) with modest ''temperature'' $T_\parallel=25$ keV, parameters which are characteristic of the Earth's outer radiation belt. Calculations have been performed for the three distinct forms for the electron distribution function specified in Section III. Each hot electron distribution has the same effective value of $\langle p_\parallel^2\rangle$, a thermal anisotropy $A=2$, and a fractional

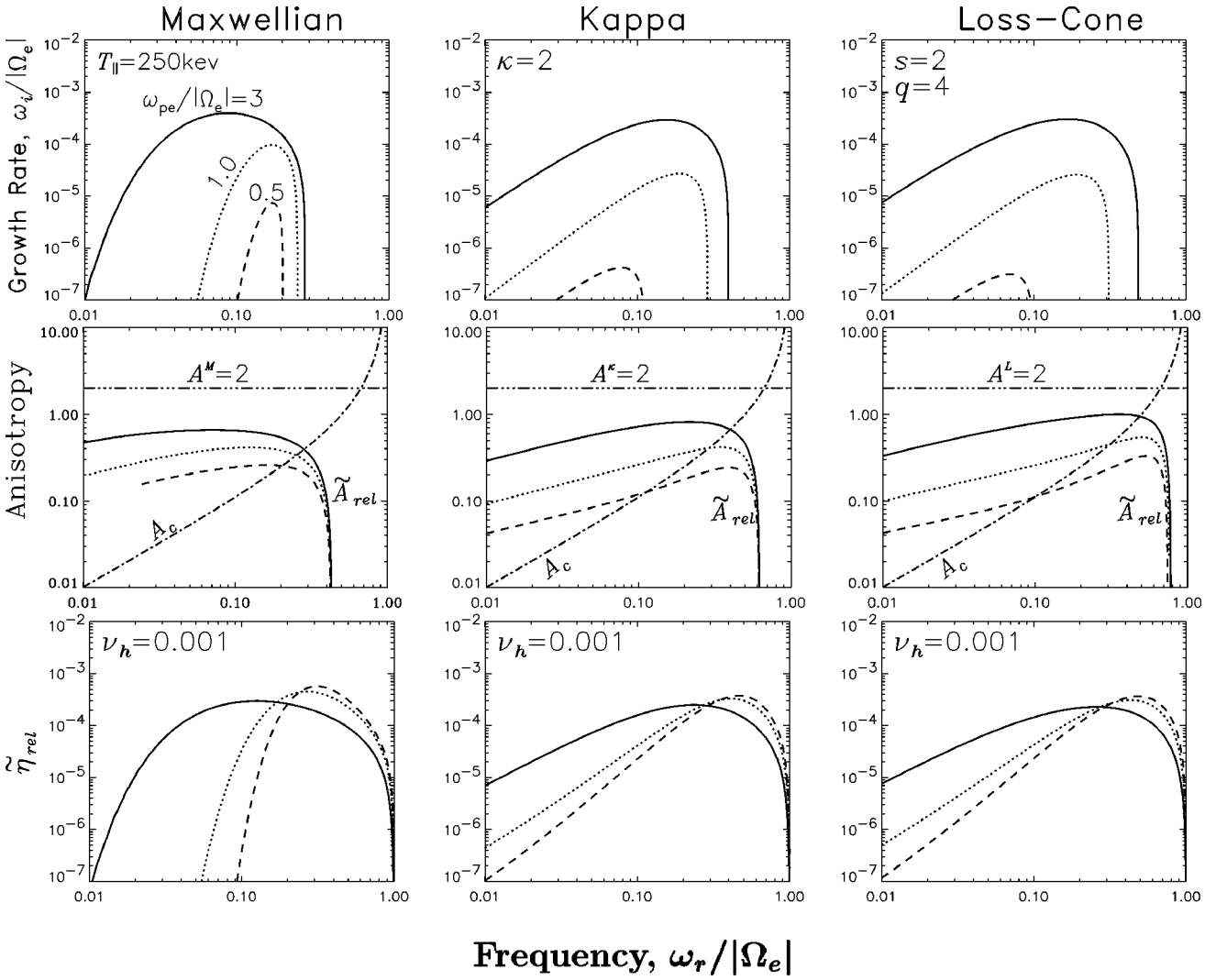

FIG. 5. Sensitivity of the fully relativistic calculations to changes in the cold plasma density.

composition of hot electrons, $\nu_h = 10^{-2}$. Results for a Maxwellian, kappa, and loss-cone distribution are shown, respectively, in the left, center, and right panels. For each distribution the fully relativistic wave growth rate (23) is shown in the top panels (solid curves), together with results obtained using the standard nonrelativistic approximation (19) (dotted) for the same plasma parameters. In agreement with the results of Gladd,[14] the fully relativistic solutions yield a smaller wave growth rate and a reduction in the upper frequency cut-off for instability. These differences can be attributed to changes in the resonant anisotropy $\tilde{A}_{rel}$ and the fractional number of resonant electrons $\tilde{\eta}_{rel}$, as shown in the center and lower panels, respectively. Under the nonrelativistic approximation, the resonant anisotropy $\tilde{A}$ given by (20) is identically equal to the adopted thermal anisotropy (shown dotted), as discussed by Summers and Thorne.[20] However, changes in the resonant condition along the relativistic resonant ellipses lead to a significant reduction in $\tilde{A}_{rel}$. Substituting the Maxwellian distribution (28) in (24) yields

$$\tilde{A}_{rel} = A^M \frac{\int_0^\infty (|\Omega_e|/\gamma_R - \omega_r) f^M(p_R, p_\perp) \dfrac{p_\perp^3}{\Delta_R} dp_\perp}{\int_0^\infty (|\Omega_e| - \omega_r) f^M(p_R, p_\perp) \dfrac{p_\perp^3}{\Delta_R} dp_\perp}. \tag{37}$$

Clearly, in the nonrelativistic limit ($\gamma_R \to 1$), $\tilde{A}_{rel} \to A^M$. However, the term $(|\Omega_e|/\gamma_R - \omega_r)$ in the numerator of (37) changes sign along the resonant ellipse when $\gamma_R > |\Omega_e|/\omega_r$. Consequently, $\tilde{A}_{rel} \leqslant A^M$. The reduction in $\tilde{A}_{rel}$ becomes most significant as $\omega_r \to |\Omega_e|$ (where $\tilde{A}_{rel}$ can become negative), and it is also important at a lower frequency where γ_R is larger. Changes in $\tilde{A}_{rel}$ are primarily responsible for the reduction in growth rate and in the upper cut-off frequency for instability which occurs when $\tilde{A}_{rel} = A_c$. Similar reasoning can also be used to account for the reduction in $\tilde{A}_{rel}$ for the generalized Lorentzian and the loss-cone distributions. In each case, the factor $(|\Omega_e|/\gamma_R - \omega_r)$ appears in the numerator for $\tilde{A}_{rel}$. We therefore conclude that the reduction in

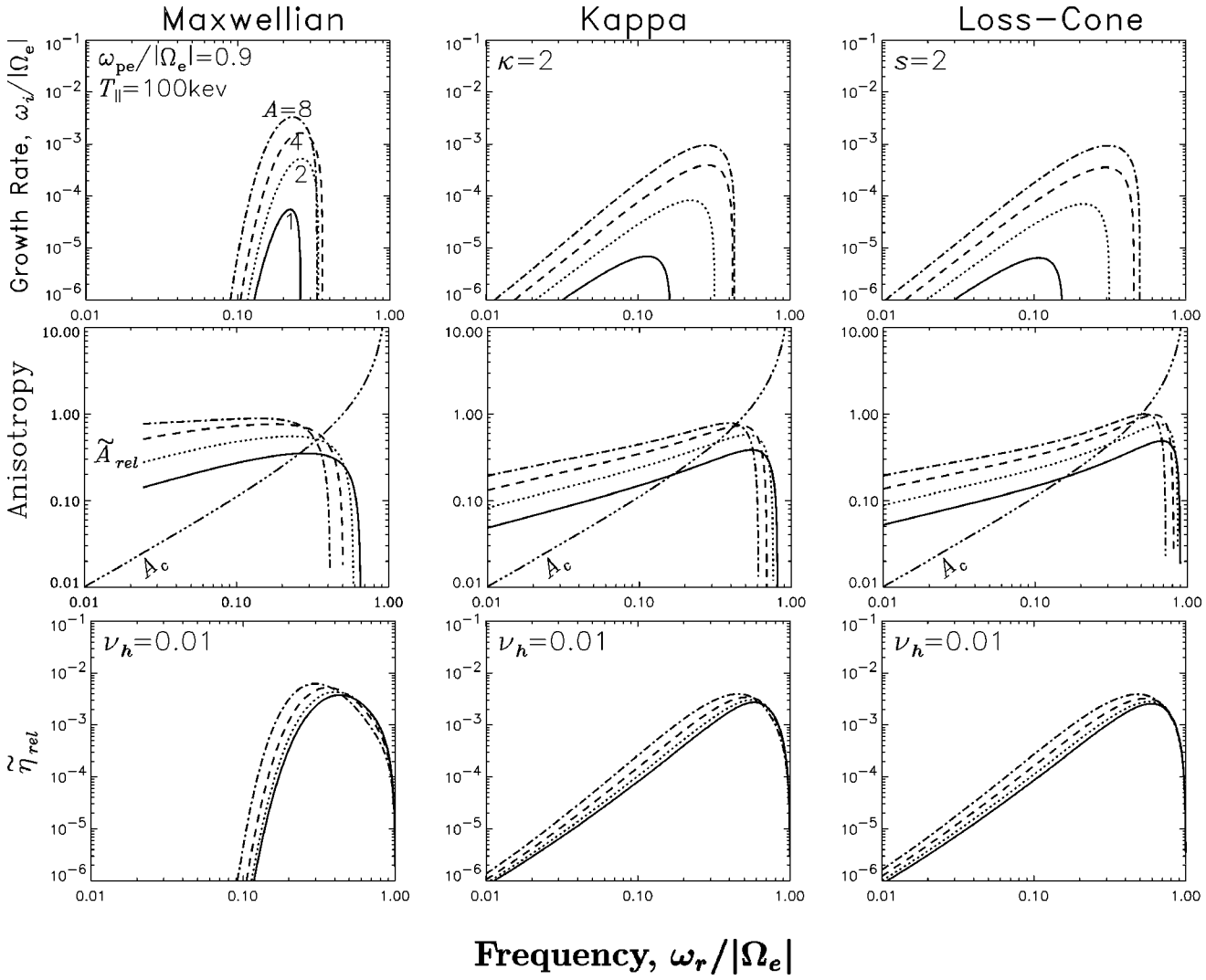

FIG. 6. Sensitivity of the fully relativistic calculations to changes in the hot electron thermal anisotropy.

wave growth is simply a consequence of relativistic effects, and that it is relatively insensitive to the exact form adopted for the hot electron distribution function.

The inner Jovian radiation belts are characterized by extremely high electron thermal energies, large pitch-angle anisotropy, and relatively low cold plasma density, $\omega_{pe}<|\Omega_e|$. In Figure 3 we show R-mode wave growth in such an environment using plasma parameters $\omega_{pe}/|\Omega_e|=0.6, T_\parallel=2.5$ MeV, $A=5$, and $\nu_h=10^{-3}$. The format of the plots is otherwise similar to that of Figure 2. The larger thermal energies, which now exceed the electron rest mass energy, lead to a pronounced reduction in $\tilde{A}_{rel}$ (middle panels) for all frequencies of interest. Relativistic resonant energies obtained from (13) are smaller than those obtained in the nonrelativistic approximation (18), and this generally leads to an increase in the fractional number of resonant electrons (lower panels). However, over the range of frequencies where wave growth is possible, the reduction in $\tilde{A}_{rel}$ is more pronounced, and this leads to a dramatic reduction in the peak wave growth rate and a pronounced drop in the upper cut-off frequency. Typically, wave growth is limited to frequencies satisfying $\omega_r \lesssim |\Omega_e|/10$ (namely in the whistler branch, $\omega_r < \omega_{pe}$), even though the adopted distribution is highly anisotropic. These results are consistent with the earlier calculation of Sentman and Goertz[9] and with the limited whistler-mode wave observations in the Jovian magnetosphere[31] which show band-limited waves at relatively low values of $\omega_r/|\Omega_e|$.

The sensitivity of wave growth to changes in the thermal energy of the resonant hot electron population is explored in Figure 4. The results are shown for all three distributions for a cold plasma with $\omega_{pe}=3|\Omega_e|$, a fractional hot electron population $\nu_h=10^{-3}$, and a hot electron thermal anisotropy $A=2$. Even for a temperature as low as 2.5 keV, relativistic effects cause a noticeable reduction in $\tilde{A}_{rel}$, both as $\omega_r \to |\Omega_e|$ and at low frequency $\omega_r \ll |\Omega_e|$. A relativistic treatment is required to evaluate the peak growth rate accurately near $\omega_r=0.5|\Omega_e|$. The relativistic corrections become more pronounced as the temperature is increased. For $T_\parallel=250$ keV, the location of both the peak wave growth (which occurs near the peak in $\tilde{\eta}_{rel}$) and the upper cut-off frequency (which occurs when $\tilde{A}_{rel}=A_c$) begin to show a dependency on the form adopted for the hot electron distribution.

Resonant interactions between electrons and R-mode waves are extremely sensitive to changes in the Alfvén speed which controls the wave phase speed. This sensitivity is explored in Figure 5 by varying the parameter $\omega_{pe}/|\Omega_e|$, for fixed hot electron parameters, $T_\parallel = 250$ keV, $A=2$, and $\nu_h = 10^{-3}$. As the cold electron density is reduced, resonant energies increase and this leads to a reduction in both $\tilde{A}_{rel}$ and $\tilde{\eta}_{rel}$ (for frequencies where wave growth is possible.) These changes lead to a dramatic drop in the wave growth rate. It should therefore be more difficult to excite whistler-mode waves when $\omega_{pe} < |\Omega_e|$. The effect would be more pronounced for a hot electron distribution with a high energy power-law tail.

For completeness, the dependence of wave growth on the adopted thermal anisotropy is shown in Figure 6. The cold plasma density is chosen with $\omega_{pe}/|\Omega_e| = 0.9$, and the hot electron population has $T_\parallel = 100$ keV and $\nu_h = 10^{-2}$. As expected, the growth rates tend to increase with A, but the relativistic effects severely limit wave growth due to the reduction in $\tilde{A}_{rel}$ as $\omega_r \rightarrow |\Omega_e|$. This tends to limit unstable waves to the range $\omega_r \lesssim 0.5|\Omega_e|$, even when $A=8$. The result should be compared to the nonrelativistic approximation for which the upper frequency cut-off is $\{A/(1+A)\}|\Omega_e| \approx 0.9|\Omega_e|$.

V. CONCLUSIONS

An explicit formula has been derived for the growth rate of electromagnetic R-mode waves in a fully relativistic plasma. The analysis is restricted to situations where the propagation characteristics of the waves are controlled solely by the cold population, and this limits its applicability to cases where the hot electron population makes a negligible contribution to the total density ($\nu_h \ll 1$), and where $\beta = 8\pi N_1 k_B T/B_0^2 \ll 1$. Relativistic effects are shown to reduce the overall wave growth rate and to reduce the upper frequency cut-off in comparison to calculations which use the nonrelativistic approximation. These effects become noticeable at relatively low thermal energy (few keV), and are a major factor for $T \lesssim 100$ keV. The principal cause of the changes from the standard nonrelativistic theory[3] is a reduction in the resonant electron anisotropy $\tilde{A}_{rel}$ which provides the source of free energy for wave instability. The reduction in $\tilde{A}_{rel}$ becomes most pronounced for $\omega_r \rightarrow |\Omega_e|$, and leads to a reduction in the upper cut-off frequency for wave instability. The change in the upper cut-off frequency and overall growth rate is more pronounced in regions of low plasma density ($\omega_{pe} \lesssim |\Omega_e|$) where resonant energies tend to be higher. This may account for the inability of waves to be excited for frequencies $\omega_r \gtrsim |\Omega_e|/10$ in the inner Jovian magnetosphere, even when the pitch-angle anisotropy is very large (e.g., Sentman and Goertz[9]).

The present analysis has been restricted to the case of waves with propagation vectors aligned along the ambient magnetic field. It should be relatively straightforward to extend the present analysis to mildly oblique waves, and then include the effects of Landau and higher-order cyclotron resonances using a technique similar to that employed by Kennel[19] for the nonrelativistic case. Extension of the theory will allow us to calculate the path-integrated gain of unducted whistler-mode waves in a relativistic plasma, and thereby quantify both the potential for waves to grow and the modification to the limiting stably-trapped flux[29] of relativistic electrons under differing magnetospheric conditions.

ACKNOWLEDGMENTS

This work is supported by National Science Foundation Grant No. ATM 97 29021, National Aeronautics and Space Administration Grant No. NAG5 4680, and North Atlantic Treaty Organization Grant No. CRG 970575. D.S. acknowledges support from the Natural Sciences and Engineering Research Council of Canada under Grant No. A-0621.

[1] L. R. Lyons, R. M. Thorne, and C. F. Kennel, J. Geophys. Res. **77**, 3455 (1972).
[2] B. Abel and R. M. Thorne, J. Geophys. Res. **103**, 2385 (1998).
[3] C. F. Kennel and H. E. Petschek, J. Geophys. Res. **71**, 1 (1966).
[4] B. A. Trubnikov, in *Plasma Physics and the Problem of Controlled Thermonuclear Reactions*, edited by M. A. Leontovich (Pergamon, New York, 1959), p. 122.
[5] I. P. Shkarofsky, Phys. Fluids **9**, 561 (1966).
[6] C. S. Wu and L. C. Lee, Astrophys. J. **230**, 621 (1979).
[7] N. Omidi and D. A. Gurnett, J. Geophys. Res. **87**, 2377 (1982).
[8] D. L. Pritchett, J. Geophys. Res. **89**, 8957 (1984).
[9] D. D. Sentman and C. K. Goertz, J. Geophys. Res. **83**, 3151 (1978).
[10] I. Lerche, Astrophys. J. **147**, 689 (1967).
[11] D. B. Melrose, *Plasma Astrophysics* (Gordon and Breach, 1980), Vol. 1.
[12] D. B. Melrose, *Instabilities in Space and Laboratory Plasmas* (Cambridge University Press, Cambridge, 1986).
[13] R. Schickeiser, H. Fichtner, and M. Kneller, J. Geophys. Res. **102**, 4725 (1997).
[14] N. T. Gladd, Phys. Fluids **26**, 974 (1983).
[15] D. C. Montgomery and D. A. Tidman, *Plasma Kinetic Theory* (McGraw-Hill, New York, 1964).
[16] C. F. Kennel and F. L. Scarf, J. Geophys. Res. **73**, 6149 (1968).
[17] S. Xue, R. M. Thorne, and D. Summers, J. Geophys. Res. **98**, 17475 (1993).
[18] D. Summers, S. Xue, and R. M. Thorne, Phys. Plasmas **1**, 2012 (1994).
[19] C. F. Kennel, Phys. Fluids **9**, 2190 (1966).
[20] D. Summers and R. M. Thorne, J. Geophys. Res. **95**, 1133 (1990).
[21] D. Summers and R. M. Thorne, Phys. Fluids B **3**, 1835 (1991).
[22] D. Summers and R. M. Thorne, J. Plasma Phys. **53**, 293 (1995).
[23] M. Bornatici, G. Chiozzi, and P. DeChiara, J. Plasma Phys. **44**, 319 (1990).
[24] K. T. Tsang, Phys. Fluids **27**, 1659 (1984).
[25] M. P. Leubner, J. Geophys. Res. **87**, 6335 (1982).
[26] H. Liemohn, J. Geophys. Res. **72**, 39 (1967).
[27] R. M. Thorne and D. Summers, Phys. Fluids **29**, 4091 (1986).
[28] R. M. Thorne and D. Summers, J. Geophys. Res. **96**, 217 (1991).
[29] D. D. Barbosa and F. V. Coroniti, J. Geophys. Res. **81**, 4531 (1976).
[30] S. R. Church and R. M. Thorne, J. Geophys. Res. **88**, 7941 (1983).
[31] D. A. Gurnett and F. L. Scarf, in *Physics of the Jovian Magnetosphere*, edited by A. J. Dessler (Cambridge University Press, Cambridge, 1983), p. 285.